ACTUATORS

Elastic energy-recycling actuators for efficient robots

Erez Krimsky[1] and Steven H. Collins[1,2]*

Electric motors are widely used in robots but waste energy in many applications. We introduce an elastic energy-recycling actuator that maintains the versatility of motors while improving energy efficiency in cyclic tasks. The actuator comprises a motor in parallel with an array of springs that can be individually engaged and disengaged, while retaining stored energy, by pairs of low-power electroadhesive clutches. We developed a prototype actuator and tested it in five repetitive tasks with features common in robotic applications but difficult to perform efficiently. The actuator reduced power consumption by at least 50% in all cases and by 97% in the best case. Elastic energy recovery, controlled by low-power clutches, can improve the efficiency of mobile robots, assistive devices, and other engineered systems.

INTRODUCTION

Electric motors have been a critical enabling technology over the past century because of their ability to efficiently convert between electrical and mechanical power in continuous processes. They now play an important role in nearly every industry and consume about 40% of all electricity produced globally (*1*). The next technological revolution will be driven by robotic systems capable of complex interactions with the environment and humans around them (*2*). These systems require dynamic control over a much wider range of torque and speed, conditions under which electric motors are far less efficient. This inefficiency limits the range of battery-powered devices, forcing the first generation of industrial quadrupeds to recharge several times per day (*3*) and hindering the adoption of the first powered prostheses (*4*). Actuators better suited to these types of tasks will make existing systems viable and enable entirely new technologies.

The strengths and weaknesses of electric motors are fundamental to their architecture. The electrical current flowing through their coils can be changed rapidly, allowing precise control of the resulting torque (*5*). The electrical resistance of these coils, however, leads to waste heat in proportion to the square of the torque under all conditions (*6*). This fundamental thermal loss applies even when producing a torque without moving or when performing tasks with equal amounts of positive and negative work, conditions that require no energy in principle. Thermal losses also limit the round-trip efficiency of energy regeneration with motors.

Unlike electric motors, mechanical springs can produce torque without consuming energy and can convert between stored elastic energy and mechanical work with near-perfect efficiency over a wide range of speeds (*7*). Adding a spring in parallel with a motor can offload some of the required torque, thereby reducing energy consumption (*8*). The resulting "parallel-elastic actuator" can even be designed to compensate for configuration-dependent loads (*9*) or such that its natural dynamics produce a desired motion (*10*).

Despite these potential advantages, parallel-elastic actuators are rarely used because of challenges in controlling their springs. A parallel spring that assists in one task may fight against the motor in a different task, increasing power consumption. Designers have addressed this issue in a variety of ways, including clutches that control spring engagement (*11*, *12*) and torque direction (*13*) and motor-driven mechanisms that adjust spring stiffness and preload (*14*). Compared with an unembellished electric motor, however, these approaches cannot reduce energy consumption without sacrificing versatility, because of either imprecise control, slow torque modulation, or high energy use in adjustment motors and clutches. If parallel spring torque could be rapidly controlled with low power consumption, large energy savings could be achieved for systems that perform many different cyclic tasks.

Energy-recycling actuator concept

Here, we describe an elastic energy-recycling actuator that combines the desirable features of both motors and springs (Movie 1). A conventional motor provides power input and fine torque control, and an array of elastomer springs provides efficient torque production and energy recovery. Low-power clutches rapidly engage and disengage springs and keep them stretched when disengaged. Spring torque is controlled by choosing which springs are engaged. We developed a prototype actuator to demonstrate these properties.

RESULTS

Prototype actuator design

We used electroadhesive clutches in our prototype actuator because they are responsive, lightweight, and very efficient. An electroadhesive clutch consists of a pair of thin, planar, dielectric-coated electrodes that slide freely past each other when deactivated and rapidly adhere when activated by applying a large voltage (*15*). Because the resulting charge is static, these clutches require hundreds of times less electrical power per unit holding torque than motors and electromagnetic clutches (*16*, *17*, *18*), which require continuous current to produce torque. Electroadhesive clutches provide a combination of rapid electronic control, low mass and volume per unit holding force, and low power to both hold force and change states while loaded, which is difficult to achieve by other means (*19*).

Each spring in the actuator is connected to two clutches: one to lock the spring to the actuator frame and another to transmit force to the joint (Fig. 1 and movie S1). The springs are planar natural rubber sheets, which exhibit low hysteresis (2 to 4% energy loss; figs. S1 and S2), store about 15 times more energy per unit mass than steel springs (*20*), and allow for a tightly stacked array when

[1]Department of Mechanical Engineering, Stanford University, Stanford, CA 94305, USA. [2]Department of Bioengineering, Stanford University, Stanford, CA 94305, USA. *Corresponding author. Email: stevecollins@stanford.edu

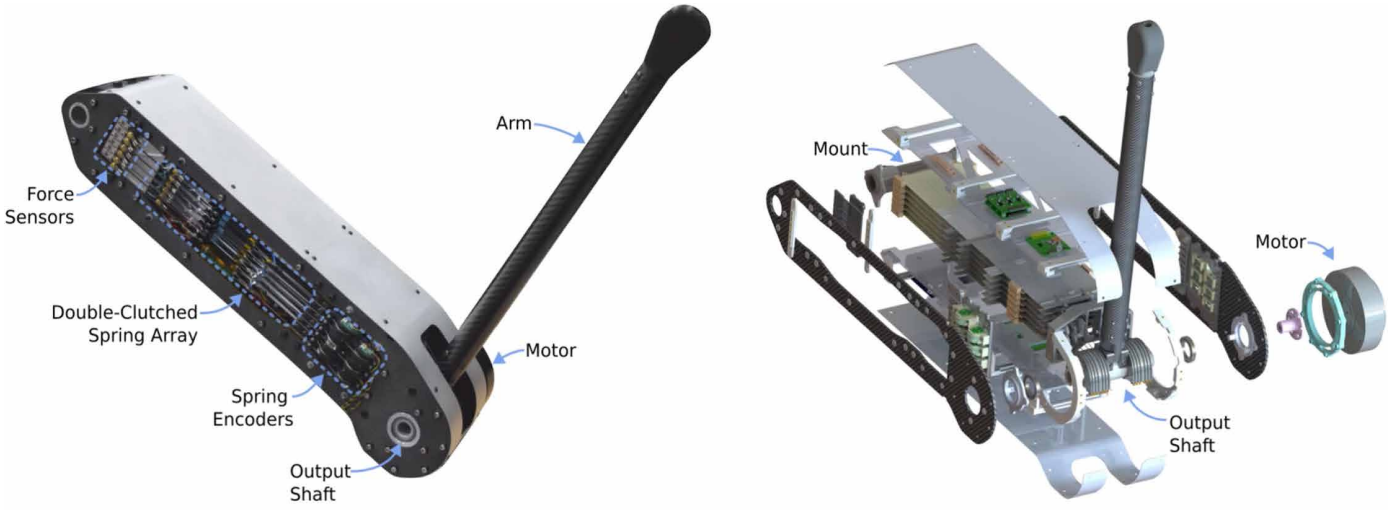

We introduce an elastic energy-recycling actuator

Movie 1.

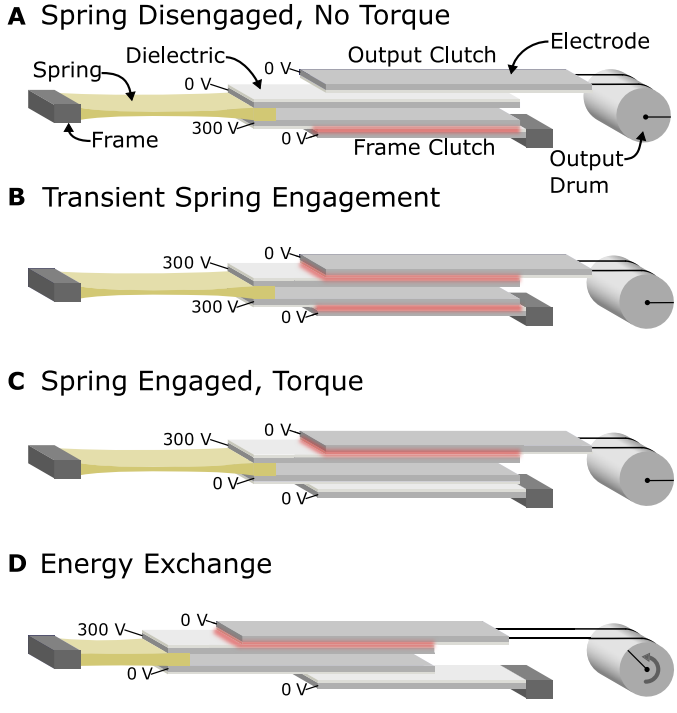

Fig. 1. Operating principle of the doubly clutched springs. Planar elastomer springs are anchored to the actuator frame on one end and connected to a frame clutch and an output clutch on the other end. (**A**) When the frame clutch is active and the output clutch is inactive, the spring is disengaged from the output and transmits its force to the frame. The spring is held in place and retains its elastic energy without applying torque to the joint. (**B**) When engaging or disengaging the spring, both clutches are active for a brief interval. (**C**) When the output clutch is active and the frame clutch is inactive, the spring is engaged and transmits force to the joint in parallel with the motor. (**D**) When engaged, the spring stretches and recoils as the joint rotates, storing and returning energy.

used with planar electrodes (figs. S3 to S6). The prototype (Fig. 2 and movie S2) uses six identical springs. Joint torque is produced by transmitting spring force through steel cables that wrap onto a drum on the output shaft (fig. S9). The mass of the clutched springs and supporting components (0.56 kg; table S1) is comparable to that of the motor and gearbox (0.49 kg) and about 21% that of the articulated arm that was actuated in our experiments (2.7 kg; table S2).

Rapidly engaging or disengaging a spring in a stretched state requires precise control of the timing of each clutch activation and deactivation. When switching states, clutch deactivation is delayed to allow time for holding force to develop in the clutch that is being activated (figs. S11 and S12).

Actuator characterization

Torque from the elastic elements can be controlled rapidly. Engaging and disengaging all springs at once produced a torque of 5.7 N·m with 90% rise and fall times of 48 ± 1 ms and 30 ± 2 ms, respectively (Fig. 3A). The delay in initial torque response (10% rise and fall times of 24 ± 1 ms and 17 ± 2 ms, respectively) is primarily due to the delays intentionally added to ensure reliable spring retention (fig. S11). The actuator can modulate the parallel-elastic torque by engaging more or fewer springs from the array (Fig. 3B and movie S3). An individual spring can be engaged and disengaged at a frequency of 12 Hz (Fig. 3C and movie S4), similar to the bandwidth of series-elastic actuators used for torque control (*21*). Torque dynamics with higher frequency content can be produced by staggering spring engagements and by controlling torque from the parallel motor.

Cyclic actuation

We evaluated the prototype energy-recycling actuator on a set of cyclic test cases with dynamics that encapsulate the relevant features of a wide range of robotic tasks. We tested sinusoidal trajectories with

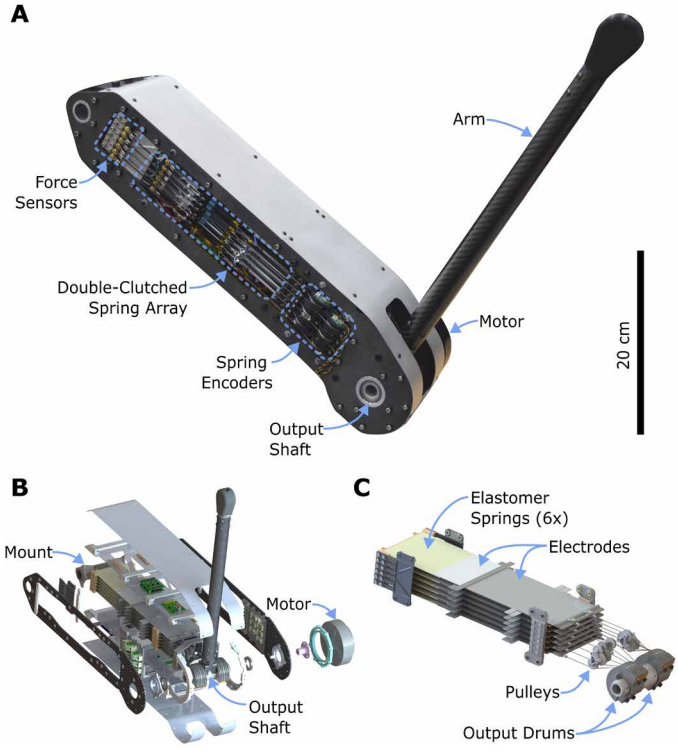

Fig. 2. Energy-recycling actuator prototype. (**A**) Photograph of the hardware prototype with six doubly clutched springs. Spring force was measured by strain gauges on the spring mounting plate. Spring displacement was measured by encoders connected to the spring-electrode tensioners (fig. S7). A geared (6:1) brushless DC motor is connected directly to the output shaft. (**B**) Exploded-view rendering showing the actuator frame (figs. S6 and S8), output shaft assembly (fig. S9), actuated arm (fig. S10), internal electronics, and other assembly components. (**C**) Rendering of the doubly clutched elastomer spring array. Cables connected to the output clutches are routed over redirection pulleys onto drums on the output shaft to produce joint torque (fig. S9).

two different masses and periods, a trajectory with rapid accelerations, a trajectory in which the payload changed mid-cycle, and a trajectory involving intermittent, forceful contact with a rigid surface (Fig. 4, movie S5, and fig. S17). To highlight the benefits of controlled parallel springs, we chose trajectories with combinations of position and torque that required no net work over the cycle. These conditions occur frequently in robotic systems, for example, when holding a static load, walking on a level surface, or picking and placing an object at the same height. In tasks with inherent positive-work requirements, energy recycling still produces benefits, although the benefits comprise a smaller portion of overall energy use.

Coordinating spring engagements to minimize energy use over long periods of time presents a challenging control problem; springs that become under- or overstretched may no longer be able to provide torque to offload the motor. For each test case, we first used offline optimization to identify desirable sequences of spring engagements, disengagements, and displacements for the preplanned trajectory (figs. S18 and S19). The objective was to minimize the difference between the nominal required torque for the task and the total spring torque while ensuring that each spring followed a cyclical trajectory and stayed within displacement limits. We posed this as a discrete-time problem, in which spring engagements and disengagements were represented by binary variables (*22*), and then solved it as a mixed-integer quadratic program (*23*). When performing the movement, we used an online feedback controller to reduce error between the nominal offline displacement and measured displacement for each spring by shifting spring engagement and disengagement times (figs. S20 and S21). For online motor control, we used a computed torque controller (*24*), incorporating estimates of parallel spring torques and the inertial and gravitational torques required for the nominal trajectory. With this approach, offline spring planning accuracy does not affect online trajectory tracking by the motor.

Dynamic trajectory testing

We compared the electrical power consumption of the energy-recycling actuator with that of a commercially available motor and gearbox. The motor, used in both systems, included an embedded control board with a dedicated microcontroller and three-phase driver chip that exhibited high baseline power consumption, about 2.4 W, even when the motor produced zero torque at rest. We did not include this baseline cost when calculating electrical energy use so as to isolate the power associated with actuation. The energy-recycling actuator used electricity to power and control its high-voltage clutches, but this cost was low: between 0.23 and 0.39 W. For each task, the actuator or motor performed closed-loop position control, achieving root mean square errors of less than 0.75° and peak error of less than 2.0° in all cases. Each experiment began with springs unstretched and the arm at its lowest position, such that no stored potential energy was initially available. Each test was conducted for 16 cycles, with data from the final 10 cycles of steady-state behavior reported. The same hardware was used for all tests.

Test cases

We first tested two simple sinusoidal trajectories with the same amplitudes but different periods and payload masses (Fig. 4, A and B). This is an example of a set of tasks for which springs can provide most of the required torque passively but only if stiffness can be varied. In this case, the faster, heavier task had twice the frequency and six times the mass. The energy-recycling actuator reduced energy consumption by 50% in the low-mass case, which required very little power, and 97% in the high-mass case, which required high power. It did so by optimizing the number of engaged springs and their displacements to match task requirements. Other approaches to adjusting spring stiffness and neutral point (*25*, *26*) could provide similar benefits but could not reduce energy consumption while producing the rapid changes in torque required for the remaining tasks.

We next tested a trajectory with step changes in acceleration of a moving load (Fig. 4C). Sharp changes in acceleration are often needed in robots, for example, when following a complex trajectory or rapidly reversing the direction of movement. The energy-recycling actuator quickly engaged and disengaged springs to switch between periods of high acceleration and deceleration, resulting in a 79% decrease in energy use. Other devices using springs and latches can reduce energy costs in tasks involving rapid acceleration from rest (*27*) but cannot produce the complex patterns of torque and movement needed to track the trajectory in this task.

We next tested a trajectory with step changes in gravitational load (Fig. 4D). Hybrid dynamics of this type occur frequently when interacting with objects or the environment (*28*). In this case, the actuated arm moved into contact with a secondary load and then advanced it along a prescribed trajectory. By engaging prestretched springs while in contact with the mass, the energy-recycling actuator

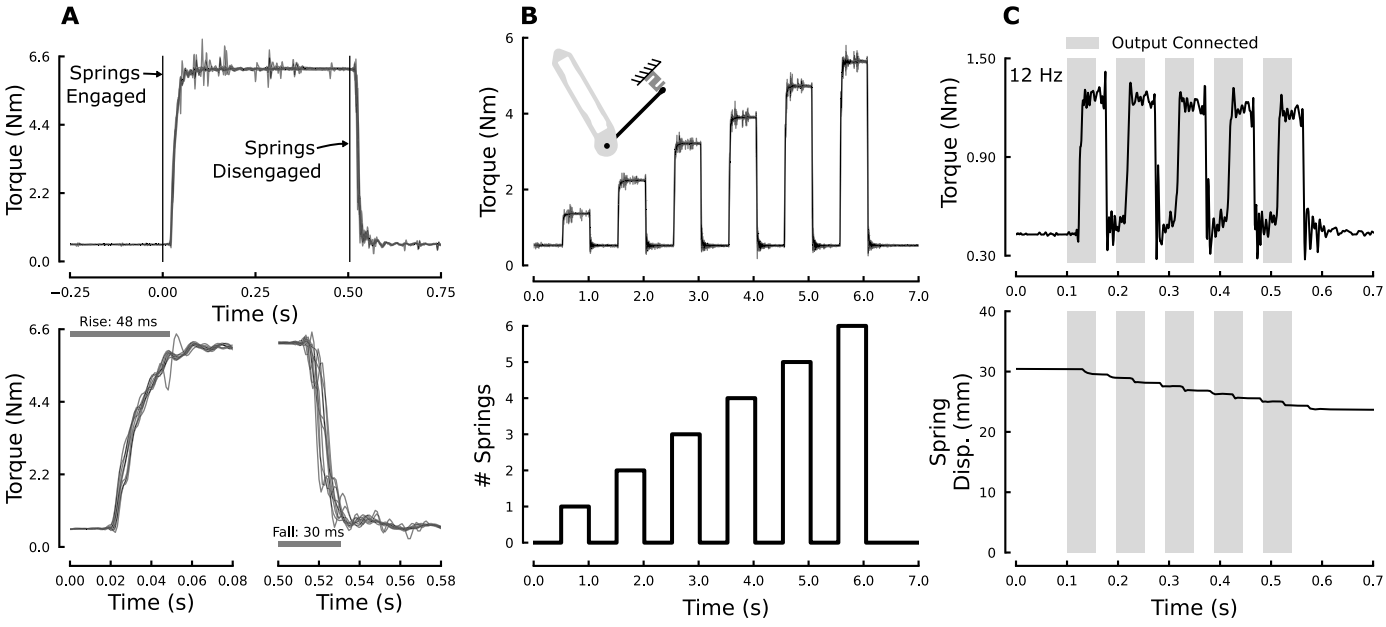

Fig. 3. Clutched spring torque response characterization. (**A**) Torque response from engaging and disengaging all springs simultaneously while under tension, demonstrating rapid rise and fall times. Data are presented from 10 consecutive tests. (**B**) Torque response from engaging different numbers of springs, demonstrating control of spring torque magnitude from among a discrete set of values. Data are presented from 10 consecutive tests. (**C**) Torque response from engaging and disengaging a single spring at 12 Hz, demonstrating high-bandwidth spring control. Torque decreases slightly with each successive engagement as clutches and cables stretch slightly and dissipate some energy (fig. S13). Joint torque was measured using a load cell at the end of the arm. In each case, springs had an initial prestretch of 30 mm, and the motor in the actuator applied a constant torque of 0.5 N·m to keep the arm in contact with the load cell when springs were disengaged.

reduced power consumption by 85%. A simple parallel spring could not produce the pattern of torque and displacement required for this task, because desired torque increases as the spring recoils. A specialized spring mechanism could be designed to provide similar energy savings (*29*) but would increase energy requirements in the other tasks.

Lastly, we tested a trajectory that included both position tracking and production of a static force against the environment (Fig. 4E). Contact with stiff surfaces, like the ground, a touchscreen, or a depressed button, requires control of contact forces without changing position. In this case, the actuated arm followed a prescribed trajectory, lightly came into contact with a load cell, applied a large force, and then lifted off. Force control was accurate for both the energy-recycling actuator and the motor, with a root mean square error of less than 3% measured by the load cell after a settling period of 75 ms (fig. S14). By engaging springs to produce most of the required static force, the energy-recycling actuator reduced power consumption by 66%. Systems that use motors to adjust parallel springs can also provide static forces economically once adjusted (*25*, *26*), but the energy required to move the spring into position would outweigh the energy saved in the motor for brief contacts like the one in this task.

Transient behavior

Although steady-state conditions are required to achieve optimal energy savings, large savings can be obtained within the first few cycles after transitioning to a new behavior. In every test case, near-optimal energy savings were achieved by the fourth cycle (Fig. 5 and fig. S15). By the second cycle, large energy savings were achieved for all but one test case (the low-mass sinusoid, which required the least motor energy to start with and therefore was most difficult to improve). During the first cycle, energy cost did not differ substantially between motor-only and energy-recycling conditions. In each test, all springs were initialized to their most relaxed state, meaning that they had no stored energy that could be used in the first cycle. In each test, the initial movement of the joint was in the direction that would have led to further shortening of the springs, meaning that the springs could not initially be used to offset motor braking torques. Under typical real-world conditions, we would instead expect a robot to be transitioning from one behavior to another, leaving springs positioned to immediately provide stored energy or assist with braking. Together, these results suggest that energy recycling will often produce large benefits, and at worst leave energy cost unchanged, within the first few cycles of a new task after transitioning from any prior task. For similar reasons, large energy savings might even be expected during sequences of unrelated single-shot movements.

DISCUSSION

Comparison with parallel elastic actuators

The energy-recycling actuator provides greater versatility than prior parallel spring mechanisms because it decouples spring torque from joint angle. There is some correlation between the required torque and position for each task we tested, but the correlation across all test cases taken together is low (Fig. 6). Linear parallel springs optimized for each task individually could reduce torque requirements in most cases, but a spring optimized across all five test cases would only reduce the mean squared torque by 64% in the best case and would increase the mean squared torque by a factor of 3 in the worst case (fig. S22) with similar effects on energy consumption (fig. S23). By dynamically adjusting spring torque independently from joint configuration, the energy-recycling actuator reduced mean squared

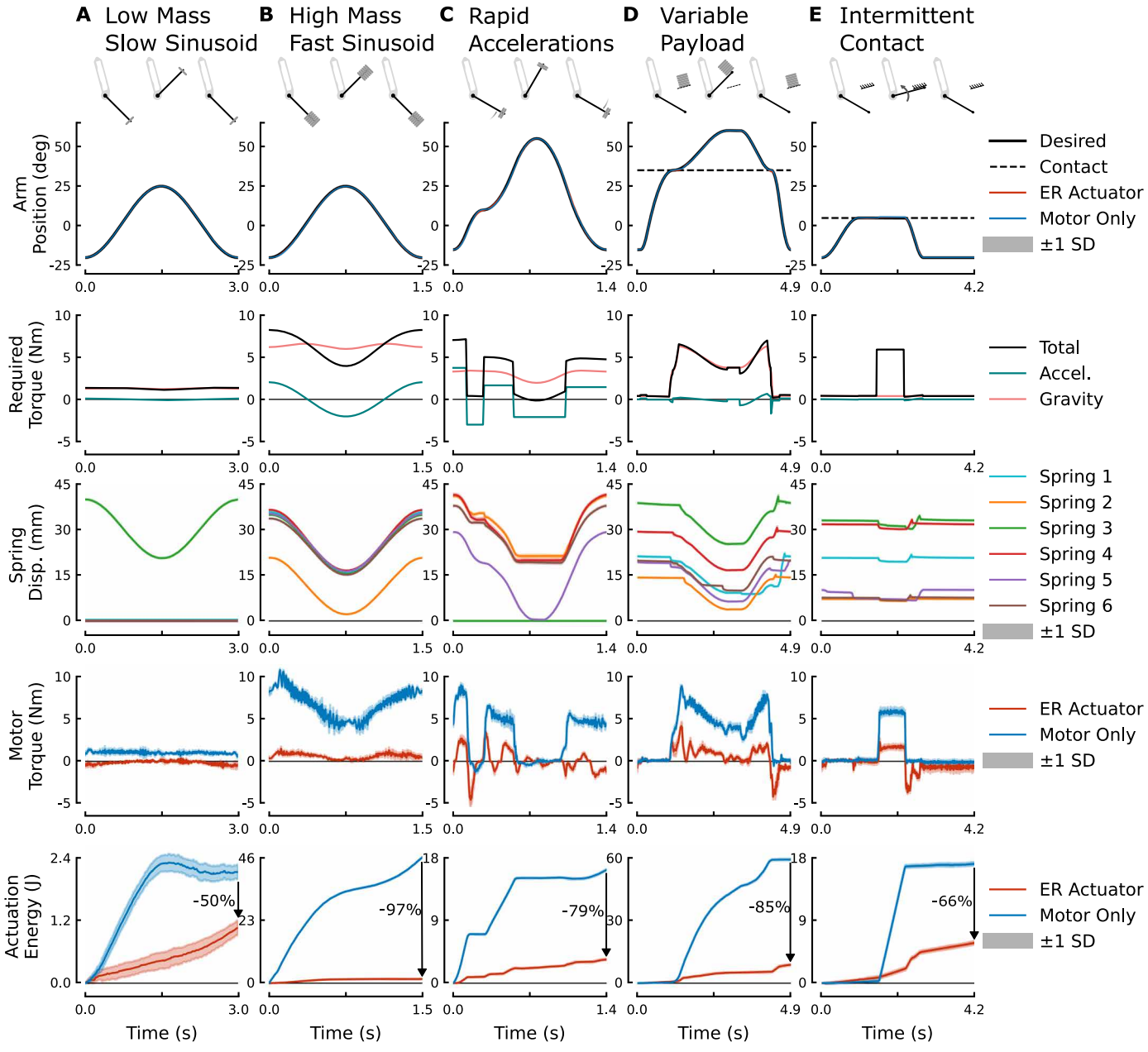

Fig. 4. Dynamic tests of actuator performance on representative tasks. Columns depict the five test cases: (**A**) slow oscillation with a small payload (0.25 kg); (**B**) fast oscillation with a large payload (1.45 kg); (**C**) rapid acceleration with a moderate payload (0.72 kg); (**D**) variable payload (0 to 1.59 kg); and (**E**) intermittent, stiff contact with force control (0 to 12.3 N; fig. S14). The top row depicts the mean ± SD of measured joint angle, which closely matched the desired values. The next row depicts model estimates of the torque required to complete each task, broken into gravitational and acceleration components. The middle row depicts measured displacement of each spring in the energy-recycling (ER) actuator. The next row depicts measured motor torque, which was substantially lower with the energy-recycling actuator than for motor-only actuation. The bottom row depicts measured energy consumption, which was substantially lower with the energy-recycling actuator in all cases. For each task, springs were initialized with zero displacement and reached steady state within 6 cycles (figs. S15 and S16). The mean and SD from the final 10 cycles are shown.

motor torque by at least 79% in all cases and by 99% in the best case. These results are consistent with our prior simulation study, which found similar reductions in torque and electrical energy consumption across 100 randomly generated task patterns (*22*).

Mechanical work and power consumption

Curiously, although the motor in the energy-recycling actuator always consumed substantially less electrical energy, it also typically performed more net mechanical work than when operating alone. The parallel springs greatly reduce motor torque (Fig. 6) and thereby electrical energy use. Each time a parallel spring is engaged or disengaged, however, a small amount of elastic energy is lost as other elements in the system stretch slightly (fig. S13). For example, each engage-disengage cycle of the bandwidth test reduced spring torque by about 5% and stored energy by about 13%. This increases the total work required to complete the task, thereby increasing the net positive

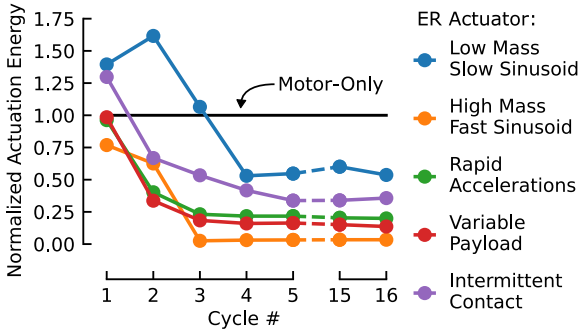

Fig. 5. Power consumption versus actuation cycle. Actuator power consumption for initial and final cycles normalized by the motor-only power consumption for each task. Steady-state power consumption was reached within the first five cycles for each task.

work the motor must produce (fig. S24). For example, in the test case with intermittent contact, net work input from the motor each cycle increased from 0.24 J for motor-only actuation to 0.93 J with the energy-recycling actuator, whereas electrical energy consumption decreased from 17 to 4 J. The small energy costs of clutching are outweighed by the large benefits of reduced motor torque and heat.

The energy-recycling actuator can reduce power consumption even for tasks that do not involve negative work. Parallel springs can be used to offload the motor during periods of static torque production, as in the intermittent contact test case (Fig. 4E). Because motor energy loss is proportional to the square of torque, the springs can even save energy by capturing and returning energy from the motor itself; energy produced economically at low torque can be stored and later used to offset expensive periods of high torque, a strategy that can be observed in the patterns of spring engagement for the variable payload task (Fig. 4D).

Variable transmission analogy

The energy-recycling actuator has functionality similar to that of a continuously variable transmission placed between a spring and a joint. In theory, such an arrangement would allow spring torque contributions to be controlled independently from spring stretch by varying the gear ratio. Unfortunately, continuously variable transmissions rely on rolling contact, which leads to unfavorable trade-offs among size, torque capacity, and shifting costs in complex cyclic applications, which we observed in preliminary work. The present design substitutes discrete changes in transmission configuration for continuous ones, resulting in a small reduction in the precision of spring torque control but a large improvement in tribological conditions. Electroadhesive clutches have almost no mass and allow springs to be engaged and disengaged for almost no energy cost, which makes it practical to include many individually controlled springs, approximating the continuous case.

Comparison with muscle

Humans use their muscles to complete complex cyclic tasks with skill and ease, and so skeletal muscle provides another interesting point of comparison for the actuator. As it happens, the two have some features in common. The clutches are either engaged or disengaged, much like the actin and myosin filaments in sarcomeres. Force control arises from the number of parallel springs engaged at a given time, analogous to selective recruitment among parallel motor units in muscle. The spring-like titin molecule in muscle may even capture and return some strain energy during repetitive movements (*30*), akin to the natural rubber springs of the actuator.

Of course, muscle exceeds the energy-recycling actuator in important ways. The actuator's functional elements are orders of magnitude larger and fewer, owing to the relative crudeness of current manufacturing capabilities. For similar reasons, whereas the energy-recycling elements have force density (1.3 kN/kg) similar to that of the human biceps brachii (*31*), their force per cross-sectional area (70 kPa) is about one-third that of muscle (*32*). And no robotic system can yet actually grow, strengthen, or heal as muscle can.

Nevertheless, the actuator outperforms muscle in several ways. When engaging, the actuator's springs develop force in a pattern similar to that of muscle (*33*) but respond about twice as fast. Unlike muscle, which consumes energy whenever tensed, the actuator can maintain static force for nearly no energy cost. It can also capture and return mechanical energy with high efficiency (figs. S1 and S2), whereas muscle expends energy to absorb mechanical work (*34*). The actuator can produce net positive work with its motor more economically than muscle, with a peak conversion efficiency of 80% (*35*) versus 25% (*34*). These results suggest that future engineered systems could use energy recycling to achieve greater speed and efficiency than humans, even in tasks for which evolution has prepared us well.

Actuator limitations and possibilities

This study demonstrates an approach that can markedly reduce energy consumption for robots, but engineering challenges remain before actuators of this type are commercially practical. The current prototype is integrated into the structure of the limb, which saves mass but makes system design challenging. It is also complex, comprising hundreds of hand-assembled components, presenting challenges for manufacture, assembly, and reliability. Modular, compact designs and robust production techniques are feasible but will need to be developed. New designs could incorporate springs with a variety of stiffnesses or elements with tunable impedance (*36*) to yield greater force resolution. Control optimization could be performed online by initializing from a library of optimal solutions. The reduced peak motor torque requirements we observed (fig. S25) mean that smaller motors could be used. Although the electroadhesive clutches used here can withstand millions of engagements and disengagements (*16*), the natural rubber springs have an expected lifetime of tens of thousands of cycles at full stretch (*37*). Alternative spring materials will be needed to achieve longevity comparable to that of electric motors.

In addition to reducing electrical power consumption, the energy-recycling actuator could greatly increase peak mechanical power output compared with motor-only actuation. In robotic and biological systems, elastic power amplification can be achieved by slowly accumulating energy in a spring and then rapidly releasing it (*38*–*40*). The doubly-clutched springs in the energy-recycling actuator could be used to provide this same functionality, allowing slow, sequential stretching of individual springs over the course of many movements followed by the rapid shortening of all springs together for maximum power. For example, a bipedal robot with energy-recycling actuators in its joints might store up spring energy over several steps and then jump over obstacles that would be insurmountable under motor power alone.

A rotary version of the energy-recycling actuator could be much more compact. The current prototype uses a rotating drum to convert the force of the springs into torque at the joint, which leads to difficult

design trade-offs. In particular, the need to maintain a minimum clutch overlap area across all spring and joint displacements tends to require long electrodes, with only a small portion used at any time. A rotary actuator comprising rotary springs and clutches (*41*) would resolve this issue; clutch overlap area and torque capacity would always be maximized, independent of spring stretch and joint angle. Rotary architectures could also simplify clutch alignment, allow bidirectional spring torque production, and enable spring power recovery in the same direction as the power was captured (*13*). In a rotary architecture, use of electroadhesive clutches with greater holding force (*17*) would lead directly to a smaller system envelope.

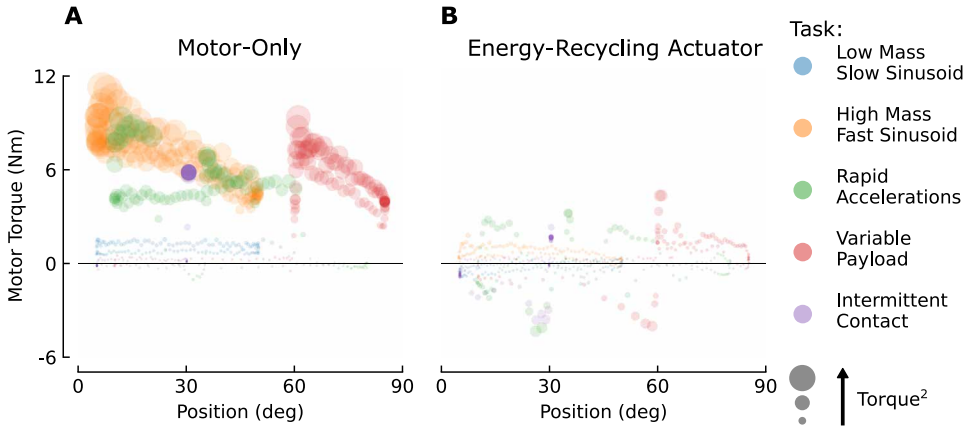

Fig. 6. Torque-position relationship for the five representative tasks. Measured electromechanical motor torque versus joint angle is shown for (**A**) motor-only actuation and (**B**) the energy-recycling actuator. The correlation between torque and joint angle across all test cases is low ($R^2 = 0.002$), which would limit the value of parallel spring mechanisms that produce torque as a function of displacement. The energy-recycling actuator selectively engages springs, decoupling spring torque from joint angle and allowing large reductions in motor torque for all cases. In this figure, test data are down-sampled to 125 points per cycle from the average over the last 10 cycles. The area of each data point is proportional to motor torque squared at that instant, which corresponds to waste heat generated by the motor. A minimum point size is set for visibility. Darker regions occur when multiple data points overlap.

Potential applications

Elastic energy-recycling actuators will allow mobile and wearable robots to operate longer in the field, overcoming the battery limitations that currently hinder adoption. For example, they could be used to power the joints of legged robots, resulting in more efficient leg swing and intermittent foot contact, incorporating features of each of the example tasks in this study (Fig. 4). The actuator could improve energy economy across a wide range of stepping frequencies (*42*), foot path trajectories (*43*), and carried loads (*44*) by adjusting the pattern of spring engagements quickly, at low energy cost, and without any hardware changes. Such transitions between gaits occur much less frequently than individual steps, even in conditions with extremely high variability (*45*), meaning that the actuator would yield near-optimal energy savings most of the time. Even during bouts of just a few steps, we would expect meaningful benefits; in our test cases, most of the energy savings were achieved by the second cycle when starting from completely relaxed springs (Fig. 5 and fig. S16). As another example, energy-recycling actuators could be used to more efficiently power the joints of upper body exoskeletons, assisting humans as they cyclically lift and lower heavy objects (*46*), move tools (*47*), position and hold workpieces (*48*), or shift between challenging postures (*49*). Again, a variety of objects, tools, positions, and postures could be accommodated simply by changing clutch control patterns, with large energy savings after only a few cycles. Similar conditions arise in many mobile and wearable robot applications, including prosthetic legs that produce rapid changes in knee flexion to ensure ground clearance on each step, following patterns that change with speed (*50*); robots that cooperatively manipulate loads with their human counterparts, periodically switching between tasks (*51*); warehouse robots that conduct pick and place operations, regularly changing objects or targets (*52*); inspection robots that trace complex architectures, intermittently switching between structures (*53*); and manufacturing robots that move to position and apply static bracing forces (*54*). In all of these applications, elastic energy recycling could yield large improvements in energy efficiency compared with electric motors.

Elastic energy recycling could also play a vital role in industries beyond mobile robotics. Medical microrobots could capture energy from natural body movements, allowing them to deliver advanced therapies indefinitely. Cars could stop and accelerate far more efficiently than with regenerative braking, leveraging the higher round-trip efficiency of elastic systems. Excess power generated by solar and wind plants at times of peak production could be stored elastically and returned at times of peak demand. Strategic use of elastic energy conversion could improve efficiency for mechanical systems across a large set of applications, enabling new technologies not yet imagined.

Conclusions

We have introduced an elastic energy-recycling actuator that combines the desirable features of motors and springs. We describe a prototype actuator that uses an electric motor to provide power input and fine torque control, an array of elastomer springs to provide efficient torque production and energy recovery, and low-power electroadhesive clutches to individually engage and disengage springs to control torque and retain stored energy. In a series of experiments, we have demonstrated that torque from the elastic elements can be controlled rapidly and that large energy savings can be achieved in cyclic test cases that encapsulate a wide range of robotic tasks. Our results show that elastic energy-recycling actuation can markedly reduce energy consumption for robots. To make this type of actuator practical, future work should develop modular, rotary versions of the hardware and control strategies that do not require offline planning.

MATERIALS AND METHODS

Materials

The electroadhesive materials used in this study were purchased from ESTAT Actuation (Pittsburgh, PA) and consisted of 50-μm-thick aluminum-sputtered Mylar (biaxially-oriented polyethylene terephthalate) sheets with a ~12-μm dielectric coating (Luxprint; DuPont Microcircuit Materials, Research Triangle Park, NC). The natural

rubber material for the springs had a 40A durometer rating and was obtained from McMaster-Carr.

Double-clutched spring design

The double-clutched spring assembly consists of a planar elastomer spring connected to two electroadhesive electrodes sandwiched by two mating electrodes. We refer to the electrodes mechanically connected to the spring as the "spring-output" electrode for the electrode that is part of an output clutch and "spring-frame" electrode for an electrode that is part of a frame clutch and refer to the other two electrodes for each spring as a "frame electrode" or "output electrode" (figs. S3 and S4). The overlap area of the electroadhesive clutches depended on spring stretch and joint angle and ranged from 16 to 102 cm^2.

Electrodes were cut to size using a handheld rotary cutter. All mechanical connections to the electrodes were made with VHB 300LSE double-sided acrylic-based adhesive from 3M. Individual springs were cut to size (89 mm by 53 mm) using a 40-W, 10,600-nm wavelength, CO_2 laser cutter that was also used to cut the fiberglass, FR4, and VHB adhesive strips for each spring. Additional clutched-spring design and fabrication details are given in the Supplementary Materials.

Electrode tensioning and alignment

A small tensioning force needs to be applied to each electrode to keep the mating electrodes aligned and to ensure that all electrodes lay flat. The spring-frame and spring-output electrodes are tensioned by steel wire ropes that spool onto spring-loaded drums to maintain tension as the spring extends (figs. S3B and S7, A to C). A short length of string was tied between holes on both sides of the spring-frame and spring-output electrode fiberglass bars to create a loop that is connected to the tensioning wire ropes via a small jewelry clasp (fig. S7C). The loop of string can slide freely in the clasps, which allows the tension to equalize between the two electrodes. The frame and output electrodes are tensioned by 1.6-mm-diameter natural rubber rods (figs. S3 and S7D). A thin strip of open-cell polyurethane foam was mounted on the back of the fiberglass bar at the end of the spring-output electrode to keep the spring electrodes separated and to maintain contact with the output and frame electrodes.

Electronics and sensing

An overview of the electrical systems in the actuator is shown in fig. S26. Low-level clutch control and communication with spring force and spring displacement sensors were performed by a Raspberry Pi 4B mounted in the bottom of the actuator. A modified Linux kernel with the PREEMPT RT patch was used to achieve reliable real-time control. A custom-designed adapter board mounted on the Raspberry Pi (fig. S27) provided power and communication for the spring force sensors and spring encoders and included four serially chained 8-bit shift registers that enabled simultaneous updating of 32 digital output pins that connected to driver boards controlling the electroadhesive clutches. High-level control was run from a host computer that communicated with the Raspberry Pi over ethernet.

Spring displacement was measured by magnetic encoders (ams OSRAM, AS5600L) on custom circuit boards (fig. S28) that read the angle of a small magnet mounted in the tensioner spools on one side of the actuator (fig. S7B). Encoder boards communicated with the Raspberry Pi over I2C, which allows multiple boards to be soldered onto the same data and power lines.

Spring force was measured by strain gauges applied to the mounting locations for each spring. For each spring, two strain gauges were configured in a diagonal Wheatstone bridge configuration and read by custom instrumentation amplifier boards (fig. S29) mounted in the top section of the actuator. The amplifier boards were read by a separate analog-to-digital converter board (fig. S30) that communicated with the Raspberry Pi over SPI. The strain gauge calibration process is detailed in the Supplementary Materials.

High-voltage clutch control

High-voltage clutch drive circuitry is detailed in figs. S31 to S33. Activated clutches are driven with an AC square wave at 300 V and 1.25 Hz to prevent the accumulation of space charge in the dielectric material, which can substantially degrade holding force and electromechanical response time (*17*, *55*). Flipping the sign of the AC control voltage for a spring that is in the process of being engaged or disengaged could lead to a holding force drop that causes the engagement or disengagement to fail. To prevent this failure mode, polarity changes were deferred for springs that were in the process of being engaged or disengaged. We also found that on a few occasions, for some of the springs in the actuator, polarity changes while a spring was actively being stretched could cause the output clutch to disconnect. To prevent these disconnections, we defined a safe polarity flip region on the basis of a combination of spring displacement and spring linear velocity and deferred the polarity flips when they could cause failure (fig. S34), leading to an effective AC frequency that may be slightly below the nominal frequency.

To prevent any adhesion between frame electrodes and output electrodes of each spring, the frame and output electrodes were electrically connected and were always driven with a 300-V square wave, even when the clutches were deactivated. Clutch activation and deactivation were performed by controlling the voltage on the spring-output and spring-frame electrodes such that when a spring electrode is driven 180° out of phase with the frame and output electrodes, it is activated, and when it is driven in phase, it is deactivated. To reduce the required number of clutch driver boards, the frame and output electrodes were grouped for springs 1 to 3 and springs 4 to 6, with each group being driven by its own board. The groups were driven 90° out of phase with each other to reduce the peak current draw from the high-voltage source.

When switching spring states for a stretched spring, we added a time delay after activating the previously inactive clutch before deactivating the previously active clutch to account for the time required for holding force to develop in clutch activation. When deactivating a clutch, we alternated between short intervals (<500 μs) when the spring electrode of the disconnecting clutch is driven in phase with the frame and output electrodes and longer intervals (~2 to 7 ms) when the spring electrode is electrically "floated," i.e., not connected to the high-voltage source or ground. This prolonged the decay of the electric field in the deactivating clutch, which slowed its release (fig. S12) and allowed the spring force to transfer more gradually between the pairs of clutches, avoiding mechanical shock loading of the newly activated clutch, which could cause it to disconnect. This sequence is summarized in a state machine given in fig. S11. Additional details are given in the Supplementary Materials.

Characterization methods

Actuator torque was measured by a load cell in contact with the point foot at the end of the actuated arm. The load cell was positioned with its axis normal to the plane of contact so that the torque was simply

the contact force multiplied by the arm length. The motor in the actuator was commanded to apply a constant 0.5 N·m to maintain contact with the load cell when the springs were disengaged. For each test, the springs were first set to a desired initial displacement of 30 mm by extending the arm with the springs engaged.

Load cell readings were amplified by a strain gauge amplifier, read by a microcontroller, and streamed to a host computer at 1 kHz. Force values were zero-phase filtered using a third-order Butterworth filter with a cutoff frequency of 200 Hz. Messages from the microcontroller were time-stamped using the microcontroller clock, which was not synced with the host computer. To time sync the load cell data with the host computer and the commands sent to the clutches, we commanded a motor torque of 4 N·m for one control cycle to produce a mechanical pulse on the load cell. This peak in the load cell data was then temporally aligned with the peak in reported motor torque.

Dynamic trajectory testing

Motor and clutch drive system source voltage and current draw were read by a microcontroller with an embedded analog-to-digital converter at 1 kHz. Voltage readings were taken using a simple resistive voltage divider that was buffered by an op amp with unity gain. Current measurements were taken using current sense amplifier boards (Texas Instruments, INA190EVM) calibrated over the range of expected currents. The output from the current sense amplifier was unity gain–buffered and fed to the microcontroller. The current and voltage measurements were low-pass filtered by the microcontroller with a second-order filter at 250 Hz and multiplied to produce a power consumption measurement. The power consumption was integrated by the microcontroller to compute a total energy consumption for both the high-voltage system and the motor. For the clutch drive system, power was measured directly from a regulated 5-V source and included the power required to step up the source voltage and regulate it to 300 V. Motor power consumption was measured directly from a 24-V benchtop power supply. Voltage, current, power, and energy measurements were streamed from the microcontroller to the host computer at ~100 Hz.

For the tests with purely inertial loads, 0.23-kg plate weights were fixed directly to the end of the actuated arm (fig. S10D). For the slow sinusoid, fast sinusoid, and rapid acceleration tests, we used one, six, and three plates, respectively. For the "variable payload" test case, seven plates were stacked on a secondary load arm whose axis of rotation was aligned with the output shaft of the actuator (fig. S17D). When the load arm was not in contact with the actuated arm, the load arm rested against a polyurethane bumper at 35° above horizontal. The actuator arm moved the load arm by coming into contact with a cantilevered extension at the end of the load arm. For the "intermittent contact" test case, a load cell was positioned to make contact with the end of the actuated arm at 5° above horizontal (fig. S17E). Additional details on the intermittent-contact case are given in the Supplementary Materials.

Data analysis

For the dynamic trajectory tests (Fig. 4), the signals for each cycle were interpolated at a consistent 200 Hz. Averages and SDs were computed on a per point basis for the last 10 actuation cycles. For the characterization tests (Fig. 3), the signals were filtered as described in the characterization methods but were plotted without averaging over multiple experiments.

Supplementary Materials

This PDF file includes:

Materials and Methods
Figs. S1 to S34
Tables S1 and S2
References (*56*–*58*)

Other Supplementary Material for this manuscript includes the following:

Movies S1 to S5
Data S1 and S2
Design Files

REFERENCES AND NOTES

1. P. Waide, C. U. Brunner, "Energy-efficiency policy opportunities for electric motor-driven systems" (Tech. Rep. 2011/07, OECD Publishing, Paris, 2011).
2. K. A. Demir, G. Döven, B. Sezen, Industry 5.0 and Human-Robot Co-working. *Proc. Comput. Sci.* **158**, 688–695 (2019).
3. J. Hecht, Robots need better batteries, *Nature Outlook*, 29 June 2023; www.nature.com/articles/d41586-023-02170-y.
4. J. Kim, J. Wensman, N. Colabianchi, D. H. Gates, The influence of powered prostheses on user perspectives, metabolics, and activity: A randomized crossover trial. *J. Neuroeng. Rehabil.* **18**, 49 (2021).
5. H. Asada, K. Youcef-Toumi, *Direct-Drive Robots: Theory and Practice* (MIT Press, 1987).
6. S. Seok, A. Wang, M. Y. Chuah, D. J. Hyun, J. Lee, D. M. Otten, J. H. Lang, S. Kim, Design Principles for Energy-Efficient Legged Locomotion and Implementation on the MIT Cheetah Robot. *IEEE/ASME Trans. Mechatron.* **20**, 1117–1129 (2015).
7. K. Loos, A. B. Aydogdu, A. Lion, M. Johlitz, J. Calipel, Strain-induced crystallisation in natural rubber: A thermodynamically consistent model of the material behaviour using a multiphase approach. *Continuum Mech. Thermodyn.* **32**, 501–526 (2020).
8. P. Beckerle, T. Verstraten, G. Mathijssen, R. Furnémont, B. Vanderborght, D. Lefeber, Series and Parallel Elastic Actuation: Influence of Operating Positions on Design and Control. *IEEE/ASME Trans. Mechatron.* **22**, 521–529 (2017).
9. J. Herder, "Energy-free systems; Theory, conception and design of statically balanced spring mechanisms," thesis, Delft University of Technology, Delft, Netherlands (2001).
10. U. Mettin, P. X. La Hera, L. B. Freidovich, A. S. Shiriaev, Parallel Elastic Actuators as a Control Tool for Preplanned Trajectories of Underactuated Mechanical Systems. *Intl J. Robot. Res.* **29**, 1186–1198 (2010).
11. D. F. B. Haeufle, M. D. Taylor, S. Schmitt, H. Geyer, A clutched parallel elastic actuator concept: Towards energy efficient powered legs in prosthetics and robotics, in *2012 4th IEEE RAS & EMBS International Conference on Biomedical Robotics and Biomechatronics (BioRob)* (IEEE, 2012), pp. 1614–1619.
12. B. Penzlin, M. E. Fincan, Y. Li, L. Ji, S. Leonhardt, C. Ngo, Design and Analysis of a Clutched Parallel Elastic Actuator. *Actuators* **8**, 67 (2019).
13. M. Plooij, M. V. Nunspeet, M. Wisse, H. Vallery, Design and evaluation of the Bi-directional Clutched Parallel Elastic Actuator (BIC-PEA), in *2015 IEEE International Conference on Robotics and Automation (ICRA)* (IEEE, 2015), pp. 1002–1009.
14. R. Van Ham, B. Vanderborght, M. Van Damme, B. Verrelst, D. Lefeber, MACCEPA, the mechanically adjustable compliance and controllable equilibrium position actuator: Design and implementation in a biped robot. *Robot. Autonom. Syst.* **55**, 761–768 (2007).
15. S. Diller, C. Majidi, S. H. Collins, A lightweight, low-power electroadhesive clutch and spring for exoskeleton actuation, in *2016 IEEE International Conference on Robotics and Automation (ICRA)* (IEEE, 2016), pp. 682–689.
16. S. B. Diller, S. H. Collins, C. Majidi, The effects of electroadhesive clutch design parameters on performance characteristics. *J. Intell. Mater. Syst. Struct.* **29**, 3804–3828 (2018).
17. R. Hinchet, H. Shea, High Force Density Textile Electrostatic Clutch. *Adv. Mater. Technol.* **5**, 1900895 (2020).
18. A. S. Chen, S. Bergbreiter, A comparison of critical shear force in low-voltage, all-polymer electroadhesives to a basic friction model. *Smart Mater. Struct.* **26**, 025028 (2017).
19. M. Plooij, G. Mathijssen, P. Cherelle, D. Lefeber, B. Vanderborght, Lock your robot: A review of locking devices in robotics. *IEEE Robot. Autom. Mag.* **22**, 106–117 (2015).
20. J. C. Perry, A. Rathod, Energy density and hysteresis comparison in natural rubber tube springs for wearable exoskeleton applications, in *2019 IEEE 16th International Conference on Rehabilitation Robotics (ICORR)* (IEEE, 2019), pp. 21–27. ISSN: 1945-7901.
21. J. W. Sensinger, R. F. Ff. Weir, Improvements to series elastic actuators, in *2006 2nd IEEE/ASME International Conference on Mechatronics and Embedded Systems and Applications* (IEEE, 2006), pp. 1–7.
22. E. Krimsky, S. H. Collins, Optimal control of an energy-recycling actuator for mobile robotics applications, in *2020 IEEE International Conference on Robotics and Automation (ICRA)* (IEEE, 2020), pp. 3559–3565.
23. A. Bemporad, M. Morari, Control of systems integrating logic, dynamics, and constraints. *Automatica* **35**, 407–427 (1999).

24. R. Paul, "Modelling, trajectory calculation and servoing of a computer controlled arm" (Tech. rep., Defense Technical Information Center, Fort Belvoir, VA, 1972).
25. B. Vanderborght, A. Albu-Schaeffer, A. Bicchi, E. Burdet, D. G. Caldwell, R. Carloni, M. Catalano, O. Eiberger, W. Friedl, G. Ganesh, M. Garabini, M. Grebenstein, G. Grioli, S. Haddadin, H. Hoppner, A. Jafari, M. Laffranchi, D. Lefeber, F. Petit, S. Stramigioli, N. Tsagarakis, M. Van Damme, R. Van Ham, L. C. Visser, S. Wolf, Variable impedance actuators: A review. *Robot. Autonom. Syst.* **61**, 1601–1614 (2013).
26. S. Wolf, G. Grioli, O. Eiberger, W. Friedl, M. Grebenstein, H. Höppner, E. Burdet, D. G. Caldwell, R. Carloni, M. G. Catalano, D. Lefeber, S. Stramigioli, N. Tsagarakis, M. Van Damme, R. Van Ham, B. Vanderborght, L. C. Visser, A. Bicchi, A. Albu-Schäffer, Variable Stiffness Actuators: Review on Design and Components. *IEEE/ASME Trans. Mechatron.* **21**, 2418–2430 (2016).
27. V. I. Babitsky, A. Shipilov, *Resonant Robotic Systems* (Springer Science & Business Media, 2003).
28. Z. Manchester, S. Kuindersma, *Robotics Research*, N. M. Amato, G. Hager, S. Thomas, M. Torres-Torriti, Eds., *Springer Proceedings in Advanced Robotics* (Springer International Publishing, 2020), pp. 985–1000.
29. L. F. v. d. Spaa, W. J. Wolfslag, M. Wisse, Unparameterized Optimization of the Spring Characteristic of Parallel Elastic Actuators, *IEEE Robot. Autom. Lett.* **4**, 854–861 (2019).
30. K. Nishikawa, Titin: A Tunable Spring in Active Muscle. *Phys. Ther.* **35**, 209–217 (2020).
31. W. M. Murray, T. S. Buchanan, S. L. Delp, The isometric functional capacity of muscles that cross the elbow. *J. Biomech.* **33**, 943–952 (2000).
32. J.-P. Rospars, N. Meyer-Vernet, Force per cross-sectional area from molecules to muscles: A general property of biological motors. *R. Soc. Open Sci.* **3**, 160313 (2016).
33. T. K. Uchida, S. L. Delp, *Biomechanics of Movement: The Science of Sports, Robotics, and Rehabilitation* (MIT Press, 2021).
34. C. J. Barclay, in *Muscle and Exercise Physiology*, J. A. Zoladz, Ed. (Academic Press, 2019), pp. 111–127.
35. T-MOTOR AK80–6, https://store.tmotor.com/goods-981-AK80-6.html.
36. Y. S. Narang, A. Degirmenci, J. J. Vlassak, R. D. Howe, Transforming the Dynamic Response of Robotic Structures and Systems Through Laminar Jamming. *IEEE Robot. Autom. Lett.* **3**, 688–695 (2018).
37. J. Wu, L. Chen, H. H. Li, B. L. Su, Y. S. Wang, Effect of Temperature on Tensile Fatigue Life of Natural Rubber. *IOP Conf. Ser.: Mater. Sci. Eng.* **389**, 012024 (2018).
38. E. W. Hawkes, C. Xiao, R.-A. Peloquin, C. Keeley, M. R. Begley, M. T. Pope, G. Niemeyer, Engineered jumpers overcome biological limits via work multiplication. *Nature* **604**, 657–661 (2022).
39. S. J. Longo, S. M. Cox, E. Azizi, M. Ilton, J. P. Olberding, R. St Pierre, S. N. Patek, Beyond power amplification: Latch-mediated spring actuation is an emerging framework for the study of diverse elastic systems. *J. Exp. Biol.* **222**, jeb197889 (2019).
40. G. M. Campbell, J. Yin, Y. Song, U. Gandhi, M. Yim, J. Pikul, Electroadhesive clutches for programmable shape morphing of soft actuators, in *2022 IEEE/RSJ International Conference on Intelligent Robots and Systems (IROS)* (IEEE, 2022), pp. 11594–11599.
41. ESTAT Actuation, www.estat.tech/rotaryclutches.
42. A. Badri-Spröwitz, A. Aghamaleki Sarvestani, M. Sitti, M. A. Daley, BirdBot achieves energy-efficient gait with minimal control using avian-inspired leg *clutching*. *Robotics* **7**, eabg4055 (2022).
43. S. Hong, Y. Um, J. Park, H.-W. Park, Agile and versatile climbing on ferromagnetic surfaces with a quadrupedal robot. *Sci. Robot* **7**, eadd101 (2022).
44. M. Hutter, C. Gehring, M. Bloesch, M. A. Hoepflinger, C. D. Remy, R. Siegwart, in *Adaptive Mobile Robotics*, A. K. M. Azad, N. J. Cowan, M. O. Tokhi, G. S. Virk, R. D. Eastman. Eds. (World Scientific, 2012), pp. 483–490.
45. O. Ossmy, J. E. Hoch, P. MacAlpine, S. Hasan, P. Stone, K. E. Adolph, Variety Wins: Soccer-Playing Robots and Infant Walking. *Front. Neurorobot.* **12**, (2018).
46. M. M. Alemi, S. Madinei, S. Kim, D. Srinivasan, M. A. Nussbaum, Effects of Two Passive Back-Support Exoskeletons on Muscle Activity, Energy Expenditure, and Subjective Assessments During Repetitive Lifting. *Hum. Factors* **62**, 458–474 (2020).
47. P. Maurice, J. Čamernik, D. Gorjan, B. Schirrmeister, J. Bornmann, L. Tagliapietra, C. Latella, D. Pucci, L. Fritzsche, S. Ivaldi, J. Babič, Objective and Subjective Effects of a Passive Exoskeleton on Overhead Work. *IEEE Trans. Neural Syst. Rehabil. Eng.* **28**, 152–164 (2020).
48. T. Schmalz, J. Schandlinger, M. Schuler, J. Bornmann, B. Schirrmeister, A. Kannenberg, M. Ernst, Biomechanical and Metabolic Effectiveness of an Industrial Exoskeleton for Overhead Work. *Int. J. Environ. Res. Public Health* **16**, 4792 (2019).
49. S. J. Baltrusch, J. H. van Dieën, C. A. M. van Bennekom, H. Houdijk, The effect of a passive trunk exoskeleton on functional performance in healthy individuals. *Appl. Ergon.* **72**, 94–106 (2018).
50. M. Tran, L. Gabert, S. Hood, T. Lenzi, A lightweight robotic leg prosthesis replicating the biomechanics of the knee, ankle, and toe joint. *Sci. Robot.* **7**, eabo3996 (2022).
51. E. Ng, Z. Liu, M. Kennedy, It takes two: Learning to plan for human-robot cooperative carrying, in *IEEE International Conference on Robotics and Automation (ICRA)* (IEEE, 2023), pp. 7526–7532.
52. D. P. Losey, M. Li, J. Bohg, D. Sadigh, Learning from my partner's actions: Roles in decentralized robot teams, in *Proceedings of the Conference on Robot Learning* (PMLR, 2020), pp. 752–765.
53. J.-K. Oh, G. Jang, S. Oh, J. H. Lee, B.-J. Yi, Y. S. Moon, J. S. Lee, Y. Choi, Bridge inspection robot system with machine vision. *Autom. Construc.* **18**, 929–941 (2009).
54. R. Hollis, R. Hammer, Real and virtual coarse-fine robot bracing strategies for precision assembly, in *Proceedings 1992 IEEE International Conference on Robotics and Automation* (IEEE, 1992), pp. 767–774.
55. T. Nakamura, A. Yamamoto, Modeling and control of electroadhesion force in DC voltage. *ROBOMECH J.* **4**, 18 (2017).
56. A. S. Huang, E. Olson, D. C. Moore, eduLCM: Lightweight Communications and Marshalling, in *2010 IEEE/RSJ International Conference on Intelligent Robots and Systems* (IEEE, 2010), pp. 4057–4062.
57. A. Cauligi, P. Culbertson, E. Schmerling, M. Schwager, B. Stellato, M. Pavone, CoCo: Online Mixed-Integer Control Via Supervised Learning. *IEEE Robot. Autom. Lett.* **7**, 1447–1454 (2022).
58. M. Rackl, Curve fitting for Ogden, Yeoh, and polynomial models, presented at the 7th International SciLab Users Conference, Paris France, 21 and 22 May 2015.

Acknowledgments: We thank J. Boerner, R. Wojno, J. Wang, and S. Diller for work on preliminary actuator prototypes; M. Raitor and G. R. Tan for guidance on the mechanical design of the actuator; ESTAT Actuation for supplying electroadhesive material for this study; K. Werling for providing use of a 3D printer with carbon fiber embedding capabilities; and M. R. Cutkosky, X. W. Gu, M. Schwager, M. Kennedy, J. Duchi, F. B. Prinz, P. Slade, J. Kim, K. Werling, R. Martin, A. Zerbe, G. R. Tan, M. Raitor, D. Miller, A. Lakmazaheri, S. Diller, K. Witte, L. Lau, P. Dhillon, S. Krimsky, and S. Spaugh for editorial suggestions. **Funding:** This material is based on work supported by the National Science Foundation under grant no. 1734449 and under the Graduate Research Fellowship Program. **Author contributions:** Conceptualization: E.K. and S.H.C. Methodology: E.K. and S.H.C. Investigation: E.K. Visualization: E.K. Funding acquisition: S.H.C. Project administration: S.H.C. Supervision: S.H.C. Writing—original draft: E.K. and S.H.C. Writing—review and editing: E.K. and S.H.C. **Competing interests:** S.H.C. is an inventor on patent US20200177109A1 held by Carnegie Mellon University. E.K. and S.H.C. are inventors on provisional application 63/469338 submitted by Stanford University. **Data and materials availability:** The data reported in this paper are provided as data S1 and data S2 and available at https://doi.org/10.5061/dryad.ttdz08m5h.

Submitted 12 July 2023
Accepted 20 February 2024
Published 20 March 2024
10.1126/scirobotics.adj7246

Science Robotics

Elastic energy-recycling actuators for efficient robots

Erez Krimsky and Steven H. Collins

Sci. Robot. **9** (88), eadj7246. DOI: 10.1126/scirobotics.adj7246

Editor's summary

Thermal loss in electric motors leads to a reduction in energy efficiency of the devices they power. Springs, on the other hand, can produce torque without consuming energy, but they are challenging to control. Krimsky and Collins have developed an actuator that combines the benefits of motors and springs, having both fine torque control and efficient energy recovery. A prototype actuator was tested in a series of cyclic test cases, demonstrating the potential to reduce energy consumption by 50 to 97% and highlighting the wide-reaching implications in the development of robotic systems with low energy consumption. —Amos Matsiko